PIEZOELECTRICS

An organic-inorganic perovskite ferroelectric with large piezoelectric response

Yu-Meng You,[1]*† Wei-Qiang Liao,[1]† Dewei Zhao,[2]† Heng-Yun Ye,[1] Yi Zhang,[1] Qionghua Zhou,[3] Xianghong Niu,[3] Jinlan Wang,[3] Peng-Fei Li,[1] Da-Wei Fu,[1] Zheming Wang,[4] Song Gao,[4] Kunlun Yang,[5] Jun-Ming Liu,[5] Jiangyu Li,[6,7]* Yanfa Yan,[2]* Ren-Gen Xiong[1]*

Molecular piezoelectrics are highly desirable for their easy and environment-friendly processing, light weight, low processing temperature, and mechanical flexibility. However, although 136 years have passed since the discovery in 1880 of the piezoelectric effect, molecular piezoelectrics with a piezoelectric coefficient d_{33} comparable with piezoceramics such as barium titanate (BTO; ~190 picocoulombs per newton) have not been found. We show that trimethylchloromethyl ammonium trichloromanganese(II), an organic-inorganic perovskite ferroelectric crystal processed from aqueous solution, has a large d_{33} of 185 picocoulombs per newton and a high phase-transition temperature of 406 kelvin (K) (16 K above that of BTO). This makes it a competitive candidate for medical, micromechanical, and biomechanical applications.
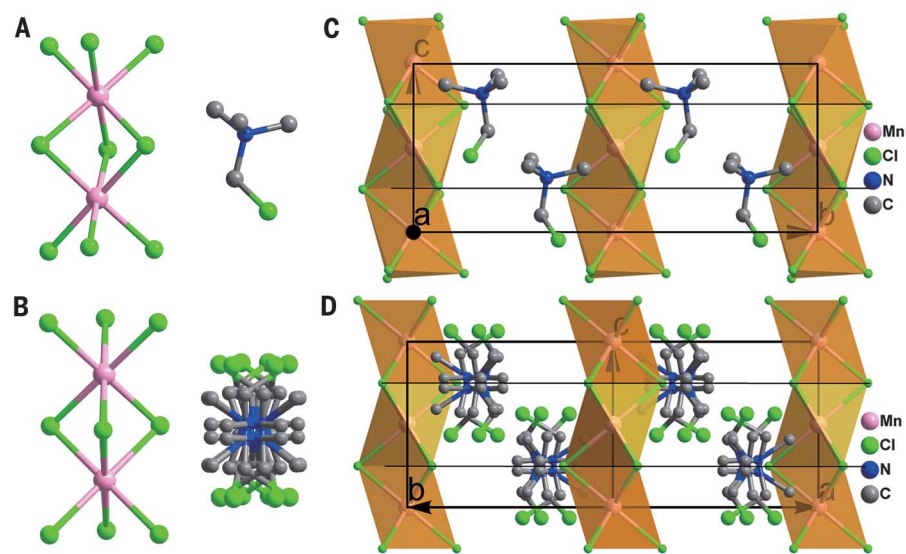
Piezoelectricity arises in crystalline materials without inversion symmetry, allowing interconversion between electric voltage and mechanical stress. This property makes piezoelectrics essential for high-voltage sources, sensors, actuators, frequency standard, motors, vibration reducer, and other applications. Pierre Curie and Jacques Curie were brothers who discovered piezoelectricity in 1880 (1). The Curies used tourmaline, quartz, topaz, cane sugar, and Rochelle salt to demonstrate the electromechanical interactions. Those first few piezoelectric materials have very weak piezoelectric performance, with piezoelectric coefficients of $d_{33} <$ 10 pC/N (2). Among these piezoelectric materials, Rochelle salt is also a ferroelectric material, discovered in 1920 by Valasek (3). Ferroelectrics feature a switchable spontaneous electric polarization and usually also have good piezoelectric performance. The most widely used piezoelectric materials currently are ferroelectric ceramics such as lead zirconate titanate (PZT) and barium titanate (BTO), which have excellent electromechanical conversion and strong spontaneous polarization.

Piezoelectric materials should be thin, soft, lightweight, flexible, and also bio-friendly for a wide variety of important applications, such as microrobotics, flexible/wearable devices, and bio-implanted sensors (4–6). These requirements impose challenges for conventional piezoelectric ceramics, which require high processing temperatures, have almost no mechanical flexibility, and contain potential toxic elements. Because these problems can potentially be solved with organic materials, organic ferroelectrics have received intensive attention (7–9). Although researchers focus on improving the spontaneous polarization (P_s) and the phase-transition temperature (T_c) (10–13) of organic ferroelectrics, the piezoresponse of organic materials still do not match that of piezoceramics such as BTO. In our previous work, we reported the largest bulk d_{33} among molecular ferroelectrics in imidazolium perchlorate (41 pC/N), yet it is only one-fifth of that of single-crystal BTO (d_{33} = 90 and 190 pC/N along [001] and [111] crystal orientation, respectively) (14, 15). Imidazolium perchlorate has an even smaller d_{33} than that of binary solid solutions such as PZT, which are as high as thousands of picocoulombs per newton with proper doping and phase engineering (5). Other organic materials have even weaker d_{33}, with ~20 pC/N for polyvinylidene fluoride (PVDF), 2 pC/N for nylon, 11 pC/N for diisopropylammonium bromide (DIPAB), and 5 pC/N for croconic acid.

Recent developments show the potential applications of organic-inorganic perovskite materials in electronics (16), light sources (17), photovoltaics (18, 19), and even ferroelectrics (20). Because of their distinct structure, hybrid materials combine the benefits of organic molecules and advantageous characteristics of crystalline inorganic solids at a molecular level. We report the discovery of a single-phase organic-inorganic perovskite piezoelectric of trimethylchloromethyl ammonium trichloromanganese(II) [Me₃NCH₂ClMnCl₃, (TMCM-MnCl₃)] that exhibits a piezoelectric coefficient

[1]Ordered Matter Science Research Center, Southeast University, Nanjing, Jiangsu 211189, P. R. China. [2]Department of Physics and Astronomy, University of Toledo, Toledo, OH 43606, USA. [3]Department of Physics, Southeast University, Nanjing, Jiangsu 211189, P. R. China. [4]College of Chemistry and Molecular Engineering, Peking University, Beijing 100871, P. R. China. [5]Laboratory of Solid State Microstructures and Innovation Center of Advanced Microstructures, Nanjing University, Nanjing 210093, P. R. China. [6]Shenzhen Key Laboratory of Nanobiomechanics, Shenzhen Institutes of Advanced Technology, Chinese Academy of Sciences, Shenzhen, Guangdong 518055, P. R. China. [7]Department of Mechanical Engineering, University of Washington, Seattle, WA 98195-2600, USA.
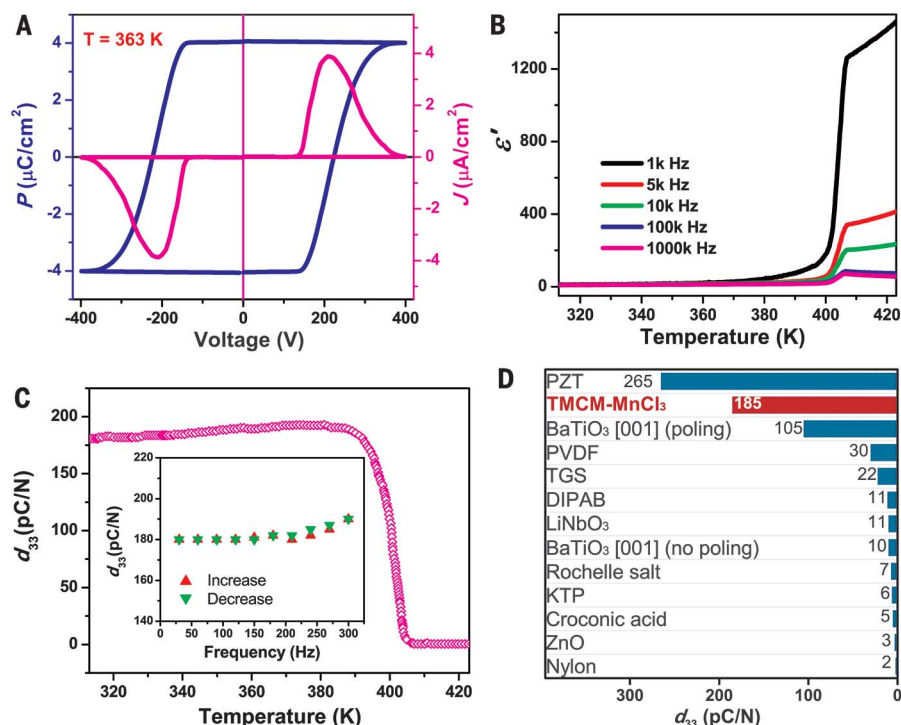*Corresponding author. Email: youyumeng@seu.edu.cn (Y.-Y.M.); jjli@u.washington.edu (J.L.); yanfa.yan@utoledo.edu (Y.Y.); xiongrg@seu.edu.cn (R.-G.X.)
†These authors contributed equally to this work.

Fig. 1. Thermal variation of crystal structures of TMCM-MnCl₃. (**A**) Structural unit of TMCM-MnCl₃ in the LTP, showing the coordination geometry of the MnCl₆ octahedron and cationic structure. (**B**) Structural unit of TMCM-MnCl₃ in the HTP, showing the multi-orientation of the cation. (**C**) Projection of the low-temperature structure. The dark lines indicate the pseudo−mirror planes normal to the c axis, which illustrate the relative ionic displacement due to symmetry-breaking. (**D**) Projection of the high-temperature structure. The dark lines indicate the mirror planes normal to the a axis. H atoms were omitted for clarity.

d_{33} of 185 pC/N. Such a large d_{33} makes TMCM-MnCl$_3$ a molecular material with a piezoelectric coefficient comparable with that of piezoelectric ceramics such as BaTiO$_3$. TMCM-MnCl$_3$ is also a high-temperature molecular ferroelectric with a T_c of 406 K (16 K above that of BTO), making it attractive for practical applications. Unlike inorganic piezoceramics, which require high-temperature synthesis and a high-voltage poling process before applications, TMCM-MnCl$_3$ is synthesized at room temperature with a preferential macroscopic ferroelectric polarization, making it suitable for growing on low-melting-point flexible substrates and fully compatible with solution-based large-area fabrication techniques. Moreover, the toxic-metal–free composition suggests that TMCM-MnCl$_3$ may be a great candidate for next-generation micro-electromechanical systems (MEMS), flexible devices, wearable devices, medical implants, and nanogenerators.

We prepared large crystals of TMCM-MnCl$_3$ in aqueous solution at room temperature (2) (figs. S1 and S2). We determined the structure with x-ray diffraction (XRD) at different temperatures (Fig. 1 and table S1). The low-temperature phase (LTP) of TMCM-MnCl$_3$ obtained at room temperature belongs to the polar space group Cc (2). The crystal packing adopts the BaNiO$_3$-like perovskite structure, similar to several other molecular ferroelectrics (21). The Me$_3$NCH$_2$Cl cation is derived from the spherical tetramethylammonium cation by replacing a H atom with a Cl atom. Typically, three-dimensional molecules such as tetramethylammonium and damantane tend to exhibit dynamical disorder in close-packed crystals because of weak van der Waals interactions. As for TMCM-MnCl$_3$, the Cl atom disturbs the spherical symmetry and thus induces the potential energy barrier to its tumbling motion. The high-temperature phase (HTP) is centrosymmetric, with the space group $P6_3/mmc$. The relationship between the two lattice cells is $\mathbf{a}^{LTP} \approx -\mathbf{a}^{HTP} - \mathbf{b}^{HTP}$, $\mathbf{b}^{LTP} \approx \mathbf{a}^{HTP} - \mathbf{b}^{HTP}$, and $\mathbf{c}^{LTP} \approx \mathbf{c}^{HTP}$ (Fig. 1A). We modeled the molecular tumbling with 12-fold orientational disorder (fig. S2). We found that in the HTP, only the N atom can be located from the difference Fourier map, indicating a strong dynamic characteristic of the molecular tumbling.

From the crystal structures of HTP and LTP, the phase-transition between these phases is induced by the order-disorder transition of the cations. In the paraelectric HTP, the crystal has a centrosymmetric structure because of the dynamic disorder of the organic cation. In the ferroelectric LTP, the crystal loses centrosymmetry because of the "freeze" of cations, which leads to the spontaneous polarization. We measured the temperature-dependent second-harmonic generation (SHG) response that supports the breaking of centrosymmetry (fig. S3). According to Aizu, this phase-transition of 6/$mmmFm$ (Aizu notation) is one of the 88 species of ferroelectrics (22). We confirmed the ferroelectricity by observing the typical polarization-electric field (P–E) hysteresis loops using the double-wave method (Fig. 2A) (23) and the Sawyer-Tower method (fig. S4).

Fig. 2. Ferroelectric and related properties of TMCM-MnCl$_3$. (**A**) Current density-bias voltage ($J \sim V$) curves and polarization-bias voltage ($P \sim V$) hysteresis loop. (**B**) Temperature-dependent data of the real part (ε') of dielectric permittivity ($\varepsilon = \varepsilon' - i\varepsilon''$, where ε'' is imaginary part of ε). (**C**) Piezoelectric coefficient (d_{33}) of TMCM-MnCl$_3$ as a function of temperature and (inset) frequency. (**D**) Piezoelectric coefficient of TMCM-MnCl$_3$ compared with some inorganic and molecular materials, including PZT, BTO, PVDF, ZnO, LiNbO$_3$, Nylon, Rochelle salt, potassium titanyl phosphate (KTP), triglycine sulfate (TGS), DIPAB (10), ImClO$_4$ (26), and croconic acid (12). Measured d_{33} values are listed at the end of each bars.

We measured the saturate polarization (P_s) of 4.0 μC/cm^2 with both methods, which corresponded well with the calculated theoretical results (fig. S5) (2). Such a polarization value is in the intermediate range among reported molecule-based ferroelectrics (9, 24). We subjected a crystal of TMCM-MnCl$_3$ to polarization switching for up to 10^7 cycles, and it showed fatigue of <10% (fig. S6).

Steplike dielectric anomalies reveal the improper ferroelectric character of the transition (Fig. 2B). We obtained a phase-transition temperature of T_c = 406 K, which is consistent with the results from several temperature-dependent measurements (fig. S3). In such an improper ferroelectric compound, the Curie-Weiss law is not applicable (25). We also measured the frequency-dependent dielectric permittivity and the imaginary part of the dielectric permittivity (figs. S8 and S9). A simple model described by the Landau-Ginzburg theory can be applied to explain the behavior of dielectric permittivity around T_c (fig. S7) (2).

Ferroelectrics are naturally piezoelectrics because of the lack of an inversion center, but most organic materials have a very weak piezoelectric response. As one of the elements in the matrix of direct piezoelectric coefficient, d_{33} represents the ability of a material to generate charges on the

plane normal to the applied strain (eqs. S1 and S2) (2). Because inorganic ferroelectrics are normally grown in the high-temperature paraelectric phase, they exhibit multidomain structures and require high-voltage poling processing before their application. Unlike inorganic ferroelectrics, crystals of TMCM-MnCl$_3$ are grown at room temperature and exhibit a nice monodomain structure (fig. S10). To measure d_{33}, we used a quasi-static method (also known as the Berlincourt method) on the as-grown single-crystal of TMCM-MnCl$_3$. In the temperature-dependent study, we obtained a maximum d_{33} of 185 pC/N along the proximity of the [102] direction of the crystal in the LTP. For temperatures above T_c, d_{33} vanishes because of the restoration of centrosymmetry, which corresponds very well with the SHG data. We also tested the piezoresponse of TMCM-MnCl$_3$ with the frequency of driving force varying from 30 to 300 Hz (Fig. 2C, inset), and this shows very little fluctuation (<10 pC/N). For a direct comparison, we measured piezoelectric coefficients of a few piezoelectric materials and several molecular ferroelectrics under the same experimental conditions (Fig. 2D and table S2). The results show that as a mono-composition ferroelectric, TMCM-MnCl$_3$ exhibits an abnormally large piezoelectric coefficient among undoped metal oxides and other molecular materials (26).

Both intrinsic and extrinsic factors contribute to the piezoelectricity. The intrinsic piezoresponse raises from the polarization change because of the lattice distortion, whereas the extrinsic factors are normally caused by the movement of non-180° domain walls or interaction between crystal grains (27). Because we obtained the macroscopic d_{33} on the as-grown single-crystalline monodomain sample, we expected the large d_{33} to be intrinsic. To further confirm the large d_{33}, we used a piezoresponse force microscopy (PFM) technique, whose submicrometer spatial resolution allows us to probe the piezoresponse within a single domain (28–31). With the sample heated up and then cooled down from the HTP paraelectric phase, the polydomain state can be obtained (figs. S11 to S15) (2). The typical PFM phase and amplitude images are shown in Fig. 3, A and B, respectively. The surface appeared as a beautiful lamellar multidomain structure. The local piezoresponse was then obtained on one of the single domains via extraction from the piezoresponse amplitude spectrum as a function of DC bias voltage, also known as a "butterfly" curve (Fig. 3C, inset, and fig. S11) (32). Such local piezoresponses obtained from LiNbO3, triglycine sulfate (TGS), BTO, and TMCM-MnCl3 were plotted as a function of macroscopic d_{33} measured with the Berlincourt method (Fig.

3C). A good linear relationship was observed. Because the local piezoresponse is proportional to the macroscopic d_{33}, the prefactor for the dependence is related to the tip-sample geometry and other factors (29), which are not in the scope of this work. From these local microscopic measurements, the observed large d_{33} on TMCM-MnCl3 can be well supported.

To explain the origin of such a large d_{33}, we need to understand the structural properties of TMCM-MnCl3. In the binary system of PZT, which is a solid solution of PbZrO3 and PbTiO3, a maximum $d_{33} > 220$ pC/N can be obtained at Zr/Ti = 0.52/0.48 by changing the relative composition of Zr. The large d_{33} is attributed to the morphotropic phase boundary between tetragonal and rhombohedral phases (33). For the single-composition crystal of TMCM-MnCl3, the large d_{33} is due to the organic-inorganic structure. Whereas the space group of the HTP of TMCM-MnCl3 is $P6_3/mmc$, the space group of LTP of TMCM-MnCl3 is the nonmaximal subgroup Cc. In this case, compared with the HTP, TMCM-MnCl3 loses more than one symmetry elements in the ferroelectric LTP, leading to the multipolar-axes characteristic, which is supported by the observation of lamellar domain structures and non-180° domain walls (Fig. 3, A and B). From
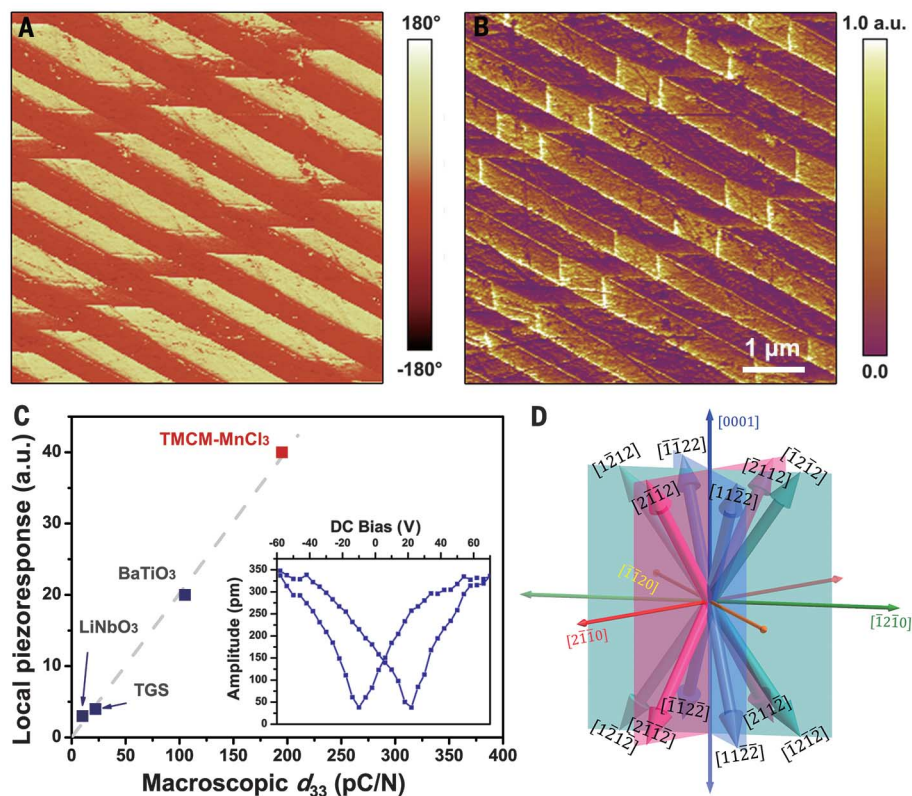
crystallographic analysis and vector-PFM analysis (figs. S12 to S14) (2), there are six polar axes in TMCM-MnCl3, resulting in 12 different polarization directions (Fig. 3D, inset). Moreover, by examining the strain tensors in the LTP, TMCM-MnCl3 is also a partially ferroelastic material (2, 22, 34). Polarization states on the same polar axis, P_i^+ and P_i^- ($i = 1, 2,..., 6$), belong to the same strain state S_i ($i = 1, 2,..., 6$). Under an external stress, materials with ferroelasticity switch from one strain state to the other, which has been intensively studied in inorganic ferroelectrics, such as BTO and PZT (35). In our case, when the external stress switches TMCM-MnCl3 from S_i to S_j ($i, j = 1, 2,..., 6$), the polarization state is also switched from $P_i^{+/-}$ to $P_j^{+/-}$ ($i, j = 1, 2,..., 6$), respectively. Such rotation of polarization direction prompts an anomalously large change of the polarization, leading to the large piezoresponsivity.

Moreover, TMCM-MnCl3 displays excellent photoluminescence properties, with a near-unity photoluminescence emission efficiency (figs. S16 to S18) (2). A thin-film sample of TMCM-MnCl3 can also be prepared with large-area coverage and good uniformity by means of a simple drop-cast method (fig. S19). The PFM characterization on domain structure and polarization reversal have also been carried out on thin-film of TMCM-MnCl3 (figs. S20 to S23) (2). Because the large piezoelectricity is due to the particular structural property, more piezoelectrics may be formed by replacing Mn with other metals. For example, we synthesized a high-temperature molecular piezoelectric compound of trimethylchloromethyl ammonium trichlorocadmium(II) [Me3NCH2ClCdCl3 (TMCM-CdCl3)] that has similarly attractive piezoelectric properties (figs. S24 to S27) (2).

We have discovered an organic-inorganic perovskite ferroelectric material of Me3NCH2ClMnCl3 (TMCM-MnCl3) that shows an excellent piezoelectric response (d_{33} = 185 pC/N) that is close to that of inorganic piezoelectrics of BTO (d_{33} = 190 pC/N) and a high transition temperature T_c of 406 K. The room-temperature process avoids the high-temperature sintering and high-voltage poling process. Solution-based processing allows deposition of TMCM-MnCl3 on various substrates, including flexible polymer, making it attractive for a variety of applications. Moreover, TMCM-MnCl3 is an organic-inorganic material that can be further engineered through element substitution and molecular design so as to optimize for a desired physical property, as shown by demonstrations of bandgap engineering (20). Combining the outstanding piezoelectric properties and application advantages of molecular materials, we believe that this class of material has great potential for the next generation of MEMS, flexible devices, wearable devices, and bionics.

Fig. 3. Microscopic ferroelectric/piezoelectric properties of TMCM-MnCl3. (**A** and **B**) Ferroelectric domain structures seen in PFM images constructed by (A) phase and (B) amplitude signal of the out-of-plane piezoresponse, where the non-180° domain structure can be clearly observed, indicating the multipolar-axes feature. (**C**) Comparison of local piezoresponse measured with PFM. The data are plotted against macroscopic d_{33} so as to demonstrate the linear dependence. (Inset) The local piezoresponse of TMCM-MnCl3 as a function of DC bias voltage. (**D**) Illustration of the 12 different polarization directions.

REFERENCES AND NOTES

1. J. Curie, P. Curie, *C. R. Acad. Sci. Paris* **91**, 294–297 (1880).
2. Materials, methods, and supplementary text are available as supplementary materials.
3. J. Valasek, *Phys. Rev.* **17**, 475–481 (1921).

4. J. Rödel et al., J. Am. Ceram. Soc. **92**, 1153–1177 (2009).
5. Y. Saito et al., Nature **432**, 84–87 (2004).
6. Z. L. Wang, J. Song, Science **312**, 242–246 (2006).
7. T. Akutagawa et al., Nat. Mater. **8**, 342–347 (2009).
8. B. Xu, S. Ren, Small **12**, 4502–4507 (2016).
9. P.-P. Shi et al., Chem. Soc. Rev. **45**, 3811–3827 (2016).
10. D. W. Fu et al., Science **339**, 425–428 (2013).
11. A. S. Tayi et al., Nature **488**, 485–489 (2012).
12. S. Horiuchi et al., Nature **463**, 789–792 (2010).
13. D. A. Bonnell, Science **339**, 401–402 (2013).
14. R. Bechmann, J. Acoust. Soc. Am. **28**, 347–350 (1956).
15. S. Wada, K. Yako, H. Kakemoto, T. Tsurumi, T. Kiguchi, J. Appl. Phys. **98**, 014109 (2005).
16. D. B. Mitzi, C. A. Feild, W. T. A. Harrison, A. M. Guloy, Nature **369**, 467–469 (1994).
17. H. Cho et al., Science **350**, 1222–1225 (2015).
18. F. Hao, C. C. Stoumpos, D. H. Cao, R. P. H. Chang, M. G. Kanatzidis, Nat. Photonics **8**, 489–494 (2014).
19. H. Tsai et al., Nature **536**, 312–316 (2016).
20. H.-Y. Ye et al., Adv. Mater. **28**, 2579–2586 (2016).
21. H.-Y. Ye et al., J. Am. Chem. Soc. **137**, 13148–13154 (2015).
22. K. Aizu, J. Phys. Soc. Jpn. **27**, 387–396 (1969).
23. L. Hu, S. Dalgleish, M. M. Matsushita, H. Yoshikawa, K. Awaga, Nat. Commun. **5**, 3279 (2014).
24. W. Zhang, R.-G. Xiong, Chem. Rev. **112**, 1163–1195 (2012).
25. A. P. Levanyuk, D. G. Sannikov, Usp. Fiziol. Nauk **112**, 561–589 (1974).
26. Y. Zhang et al., Angew. Chem. Int. Ed. **53**, 5064–5068 (2014).
27. D. Damjanovic, Rep. Prog. Phys. **61**, 1267–1324 (1998).
28. D. A. Bonnell, S. V. Kalinin, A. Kholkin, A. Gruverman, MRS Bull. **34**, 648–657 (2009).
29. A. L. Kholkin, S. V. Kalinin, A. Roelofs, A. Gruverman, in Scanning Probe Microscopy: Electrical and Electromechanical Phenomena at the Nanoscale, S. Kalinin, A. Gruverman, Eds. (Springer New York, 2007), pp. 173–214.
30. H. Lu et al., Adv. Mater. **27**, 7832–7838 (2015).
31. D. A. Bonnell et al., Rev. Mod. Phys. **84**, 1343–1381 (2012).
32. M. E. Caspari, W. J. Merz, Phys. Rev. **80**, 1082–1089 (1950).
33. W. Heywang, K. Lubitz, W. Wersing, Piezoelectricity: Evolution and Future of a Technology (Springer, 2008).
34. N. Setter, E. L. Colla, Ferroelectric Ceramics: Tutorial Reviews, Theory, Processing, and Applications (Birkhauser, 1993).
35. J. L. Jones, M. Hoffman, J. E. Daniels, A. J. Studer, Physica B **385–386**, 100–102 (2006).

SUPPLEMENTARY MATERIALS

Science

An organic-inorganic perovskite ferroelectric with large piezoelectric response

Yu-Meng You, Wei-Qiang Liao, Dewei Zhao, Heng-Yun Ye, Yi Zhang, Qionghua Zhou, Xianghong Niu, Jinlan Wang, Peng-Fei Li, Da-Wei Fu, Zheming Wang, Song Gao, Kunlun Yang, Jun-Ming Liu, Jiangyu Li, Yanfa Yan and Ren-Gen Xiong

Finding a more flexible mechanical sensor

Piezoelectric materials allow conversion between electricity and mechanical stresses. The most efficient piezoelectric materials are ceramics such as $BaTiO_3$ or $PbZrO_3$, which are also extremely stiff. You *et al.* identified an organic perovskite structured piezoelectric material that is far more pliable yet has a piezoelectric response similar to that of traditional ceramics. This material may be a better option to use as a mechanical sensor for flexible devices, soft robotics, biomedical devices, and other micromechanical applications that benefit from a less stiff piezoelectric material.
Science, this issue p. 306

ARTICLE TOOLS	http://science.sciencemag.org/content/357/6348/306
SUPPLEMENTARY MATERIALS	http://science.sciencemag.org/content/suppl/2017/07/20/357.6348.306.DC1
REFERENCES	This article cites 64 articles, 4 of which you can access for free http://science.sciencemag.org/content/357/6348/306#BIBL
PERMISSIONS	http://www.sciencemag.org/help/reprints-and-permissions

Use of this article is subject to the Terms of Service